

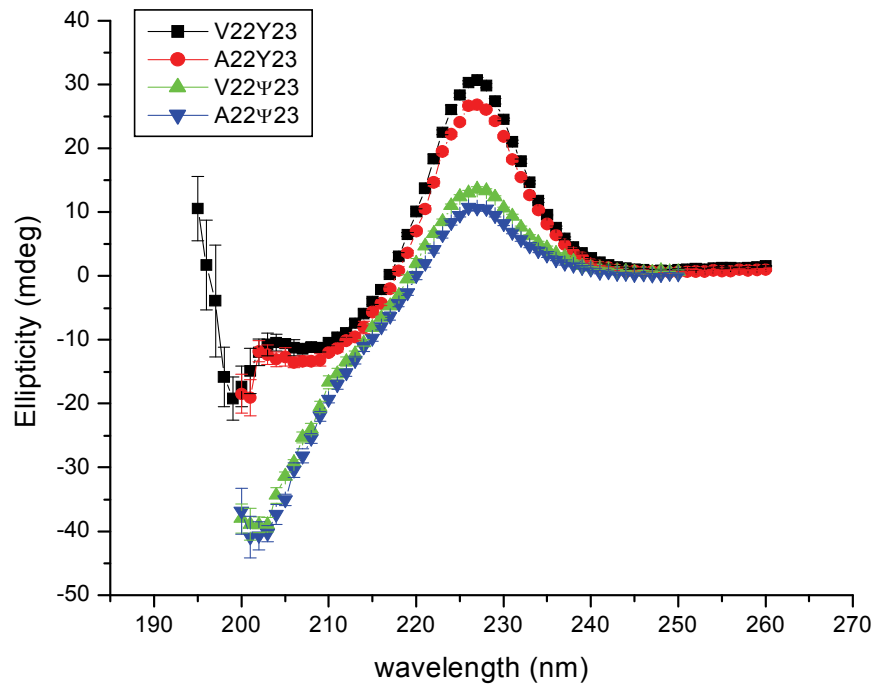
Supplementary Information for “Localized Thermodynamic Coupling
between Hydrogen Bonding and Microenvironment Polarity
Substantially Stabilizes Proteins”

Jianmin Gao, Daryl A. Bosco, Evan T. Powers*, and Jeffery W. Kelly*

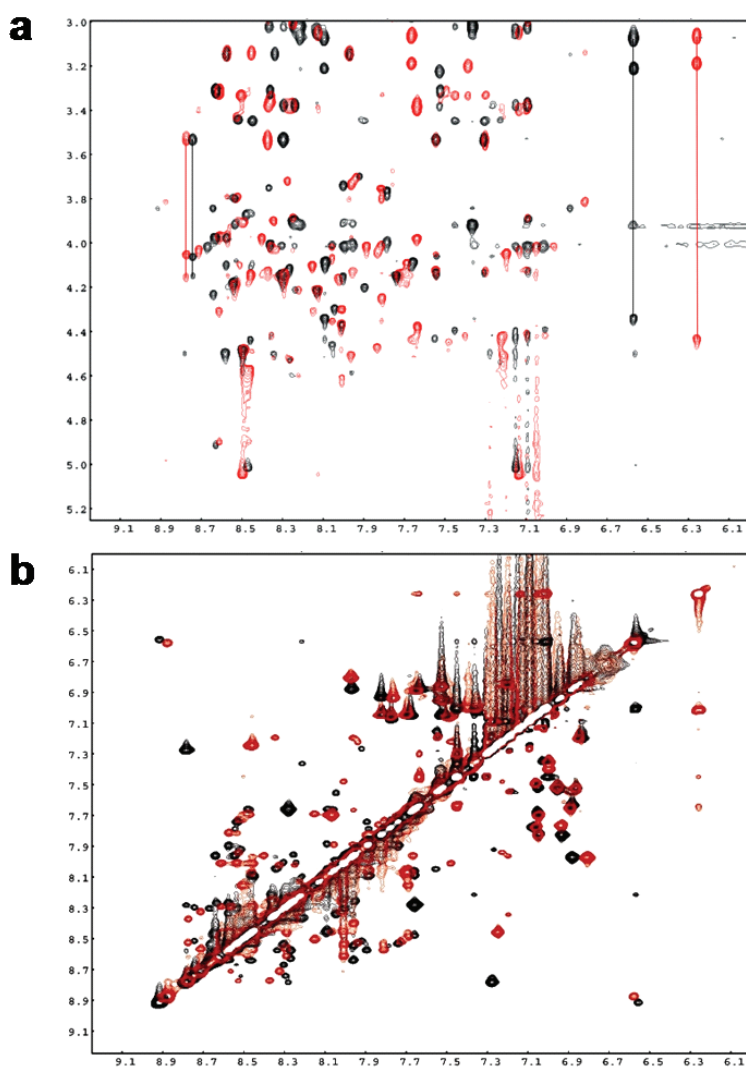
Departments of Chemistry and Molecular and Experimental Medicine and The
Skaggs Institute for Chemical Biology, The Scripps Research Institute, 10550 North
Torrey Pines Road, BCC265, La Jolla, CA 92037, USA

*To whom correspondence should be addressed. E-mail: jkelly@scripps.edu,
epowers@scripps.edu

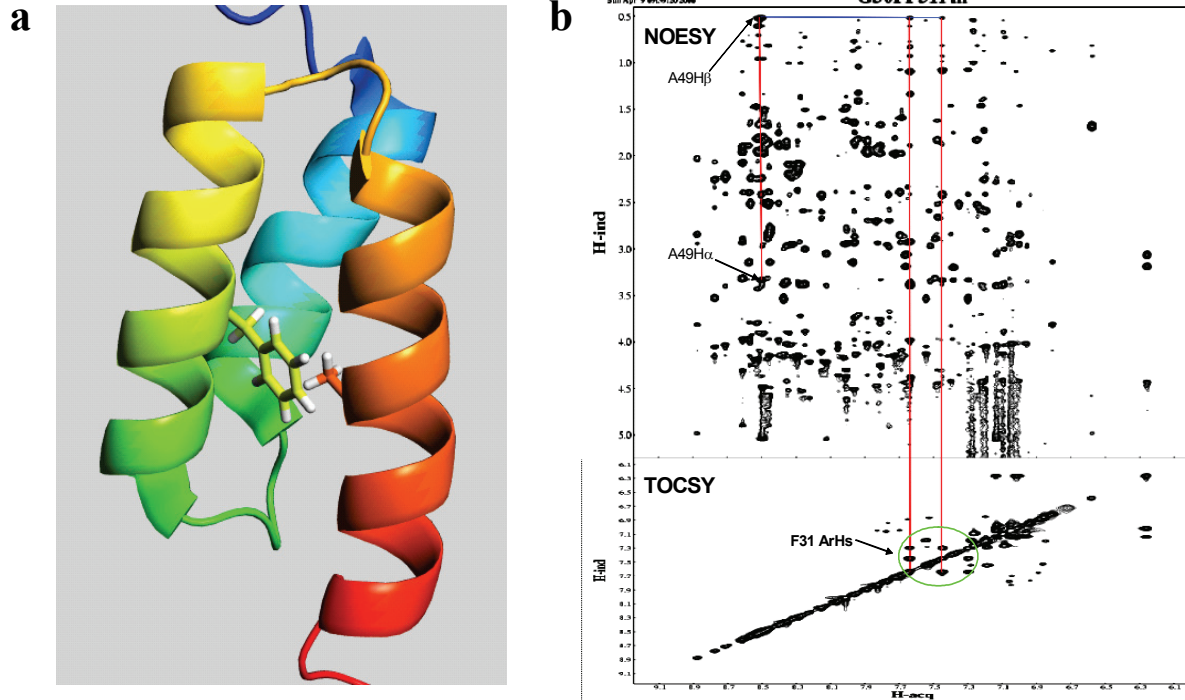
Supplementary Figure 1. Circular dichroism spectra of loop-1–modified Pin WW domain variants. The characteristic maxima were observed for all variants, indicating that they adopt a native WW domain fold.



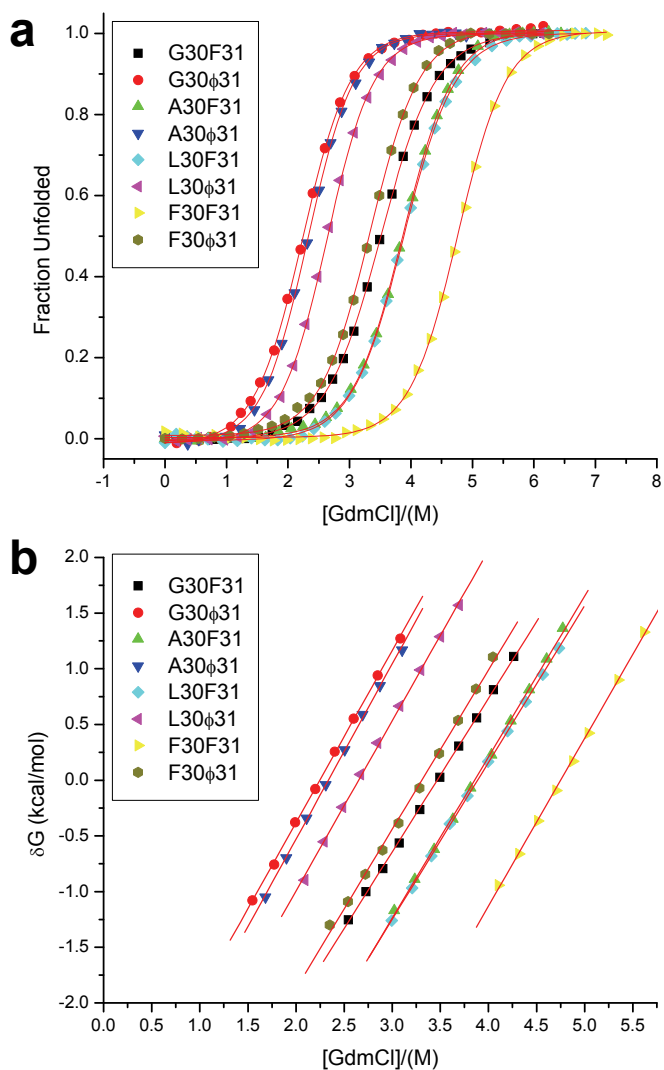
Supplementary Figure 3. ^1H - ^1H NOESY spectra of protein A* variants G30F (black) and G30F/F31 ϕ (red). (a) NH-H α region. (b) NH-NH region. The fact that G30F and G30F/F31 ϕ exhibit analogous patterns in the fingerprint regions of their 2D NOESY spectra suggests that the ester mutant G30F/F31 ϕ adopts the same structure as the all amide variant G30F. The axes in both (a) and (b) are ^1H chemical shifts in p.p.m.



Supplementary Figure 4. ^1H - ^1H NOESY data for protein A* variant G30F/F31 ϕ . (a) Native protein A structure exhibiting the signature contact between Phe31 and Ala49 side chains. (b) Combining NOESY and TOCSY allows NOESY cross peak assignment. Cross peaks between aromatic protons of Phe31 and β -protons of Ala49 indicates that this interaction, which is characteristic of the native state, is present in the G30F/F31 ϕ variant of protein A*. The axes in (b) are ^1H chemical shifts in p.p.m.



Supplementary Figure 5. Denaturation analysis of protein A* variants. (a) Guanidine hydrochloride denaturation curves of protein A* variants showing two-state cooperative transitions. (b) Thermodynamic data were extracted from fitting the denaturation curves according to a two-state model and are summarized in Table S1.



Supplementary Table 1. Summary of thermodynamic data for the protein variants used in this study. C_m is the denaturant concentration at which the protein in question is 50% unfolded and the m value is the slope of a plot of ΔG_f vs. the concentration of denaturant.

Protein	variants	C_m (M)	m values (kcal mol ⁻¹ M ⁻¹)	$-\Delta G_f$ (kcal mol ⁻¹)
Protein A*	Wild-type (A1)	3.51±0.01	1.38±0.01	4.78±0.03
	F31φ (E1)	2.24±0.01	1.54±0.02	3.47±0.03
	G30A (A2-A)	3.87±0.01	1.44±0.02	5.58±0.05
	G30A/F31φ (E2-A)	2.32±0.01	1.57±0.02	3.67±0.04
	G30L (A2-L)	3.88±0.01	1.41±0.01	5.47±0.02
	G30L/F31φ (E2-L)	2.44±0.01	1.53±0.02	3.77±0.06
	G30F (A2-F)	4.76±0.01	1.49±0.02	7.15±0.06
	G30F/F31φ (E2-F)	3.33±0.01	1.43±0.03	4.73±0.07
Loop-1–modified Pin WW domain	V22A (A1)	4.64±0.02	0.99±0.01	4.58±0.01
	V22A/Y23ψ (E1)	1.47±0.02	1.04±0.02	1.52±0.02
	Wild-type (A2)	5.85±0.02	0.99±0.02	5.65±0.11
	Y23ψ (E2)	1.52±0.03	0.92±0.03	1.42±0.05
Pin WW domain	Wild-type (A1)			3.32±0.1 [†]
	W11ω (E1)			2.20±0.05 [†]
	G30DF (A2)	3.34±0.02	1.04±0.02	3.47±0.04
	G30DF/W11ω (E2)	2.11±0.02	1.12±0.01	2.34±0.04

[†] From Deechongkit et al. *J. Am. Chem. Soc.* **126**, 16762-16771 (2004).

Supplementary Table 2. Summary of perturbation energies and backbone solvent accessible surface areas from amide-to-ester mutants in the literature. Only mutants in which the perturbed amide donates, but does not accept, a hydrogen bond are included (type 3 mutants according to the nomenclature of Powers *et al.*¹).

Protein	Mutation	Backbone exposed surface area (\AA^2) ^a	Fractional backbone exposure	$\Delta G_{f,wt} - \Delta G_{f,mut}$
Pin WW domain ^{2,3} (pdb ID: 2KCF)	W11 ω	22.4	0.53 (exposed)	-1.1
	E12 ϵ	5.0	0.11 (buried)	-1.5
	R14 ρ	5.4	0.12 (buried)	-3.9
	S16 σ	16.6	0.40 (exposed)	-1.1
	S19 σ	32.5	0.77 (exposed)	-0.6
	Y23 ψ	0.4	0.01 (buried)	-2.2
	N30 ν	17.7	0.39 (exposed)	-1.8
	A31 α	13.1	0.28 (exposed)	-0.8
	Q33 θ	4.9	0.11 (buried)	-3.1
T4 lysozyme (pdb ID: 2LZM) ⁴	(I)L50 λ	28.4	0.68 (exposed)	-0.7
Eglin C (pdb ID: 1EGL) ⁵	G70 γ	20.7	0.24 (exposed)	-0.4
P22 Arc repressor (pdb ID: 1MYK) ⁶	L8 λ	5.8	0.14 (buried)	-1.2
V9F mutant of villin headpiece (pdb ID: 1YRF) ⁷	F10 ϕ	10.2	0.24 (exposed)	-1.5
Protein L (pdb ID: 1HZ6) ⁸	F106 ϕ	1.8	0.04 (buried)	-0.55
Average, buried sites	n/a	n/a	≤ 0.2	-2.1 ± 0.5
Average, exposed sites	n/a	n/a	> 0.2	-1.0 ± 0.2

^aExposed surface areas were calculated using the program GETAREA⁹.

Supplementary References

1. Powers, E.T., Deechongkit, S. & Kelly, J.W. Backbone-backbone H-bonds make context-dependent contributions to protein folding kinetics and thermodynamics: Lessons from amide-to-ester mutations. *Adv. Protein Chem.* **72**, 39-78 (2006).
2. Deechongkit, S., Dawson, P.E. & Kelly, J.W. Toward assessing the position-dependent contributions of backbone hydrogen bonding to beta-sheet folding thermodynamics employing amide-to-ester perturbations. *J. Am. Chem. Soc.* **126**, 16762-16771 (2004).
3. Deechongkit, S. et al. Context-dependent contributions of backbone hydrogen bonding to beta-sheet folding energetics. *Nature* **430**, 101-105 (2004).
4. Koh, J.T., Cornish, V.W. & Schultz, P.G. An experimental approach to evaluating the role of backbone interactions in proteins using unnatural amino acid mutagenesis. *Biochemistry* **36**, 11314-11322 (1997).
5. Lu, W.Y. et al. Deciphering the role of the electrostatic interactions involving Gly70 in eglin C by total chemical protein synthesis. *Biochemistry* **39**, 3575-3584 (2000).
6. Wales, T.E. & Fitzgerald, M.C. The energetic contribution of backbone--backbone hydrogen bonds to the thermodynamic stability of a hyperstable P22 Arc repressor mutant. *J Am Chem Soc* **123**, 7709-7710 (2001).
7. Gao, J.M. & Kelly, J.W. Toward quantification of protein backbone-backbone hydrogen bonding energies: An energetic analysis of an amide-to-ester mutation in an alpha-helix within a protein. *Protein Sci.* **17**, 1096-1101 (2008).
8. Yang, X., Wang, M. & Fitzgerald, M.C. Direct analysis of backbone-backbone hydrogen bond formation in protein folding transition states. *J Mol Biol* **363**, 506-519 (2006).
9. Fraczkiewicz, R. & Braun, W. Exact and efficient analytical calculation of the accessible surface areas and their gradients for macromolecules. *J. Comput. Chem.* **19**, 319-333 (1998).